View Online / Journal Homepage / Table of Contents for this issue

J. CHEM. SOC. FARADAY TRANS., 1995, 91(12), 1813–1824

Cation Location and Migration in Lanthanum-exchanged Zeolite NaY studied by X-Ray Powder Diffraction and MAS NMR spectroscopy

Harald Klein† and Hartmut Fuess*
Fachgebiet Strukturforschung, Fachbereich Materialwissenschaft, Technische Hochschule Darmstadt, Petersenstrasse 20, D-64287 Darmstadt, Germany
Michael Hunger
Institut für Technische Chemie I, Universität Stuttgart, D-70550 Stuttgart, Germany

The population of cation sites in a lanthanum-exchanged zeolite NaY (LaNaY-73) in the course of calcination and at conditions similar to catalysis ($T = 623$ K, continuous flow of *m*-xylene and nitrogen over calcined zeolite LaNaY) has been studied by *ex situ* and *in situ* X-ray powder diffraction. *Ex situ* magic-angle spinning (MAS) NMR spectroscopy at room temperature complemented the diffraction results. During calcination of LaNaY, a cation migration process (lanthanum from supercage to sodalite cage, sodium from sodalite cage to supercage), after pretreatment at 363 K, was observed. In the calcined sample all lanthanum cations are located at position SI′ in the sodalite cage while 10 of the 16 sodium cations per unit cell occupy position SII in the supercage. A sodium migration from the sodalite cages to position SII in the supercages was observed by *ex situ* temperature-dependent experiments on samples calcined between 298 and 623 K. X-Ray powder diffraction, as well as multinuclear solid-state NMR spectroscopy, has shown that adsorption of *m*-xylene induces sodium migration from the sodalite cages to position SII in the supercage, whereas the positions of lanthanum are not influenced. Furthermore, *m*-xylene could be located by *in situ* X-ray powder diffraction at conditions similar to catalysis at the preferred adsorption site in front of the six-ring window of the supercage, as determined by *ex situ* diffraction experiments at low temperature. The positions and populations of the cations derived at 623 K agree with the results obtained from *ex situ* diffraction experiments carried out at this temperature.

Published on 01 January 1995 on http://pubs.rsc.org | doi:10.1039/FT9959101813
Downloaded by Universitat Stuttgart on 20 June 2012

The exchange of lanthanum *vs.* sodium in zeolite NaY produces an acidic catalyst of high thermal stability after calcination, which is extensively used in petroleum-refining processes.[1,2] In hydrated as-exchanged zeolites LaNaY, all La^{3+} cations are located in the supercage.[3–5] During the calcination process, the La^{3+} ions partially strip off their hydration shell and migrate from cation positions in the supercage to position SI′ in the sodalite cage.[4–11] The Brønsted acid sites, determined by IR[12] and neutron diffraction[9] studies, are generated by the hydrolysis of water molecules on the rare-earth-metal cations. The thermal stability of zeolite LaNaY was attributed to hypothetical lanthanum clusters[10,12,13] in the sodalite cages, consisting of at least two lanthanum cations connected by bridging oxygen or hydroxide ligands. The existence of such clusters, however, is controversially discussed in the literature, because neutron powder diffraction studies[9] revealed single La^{3+} cations coordinated to framework oxygen and to one terminal extra-framework hydroxy group.

Although the migration of lanthanum cations from supercage to sodalite cage is generally acknowledged, the behaviour of the cations after adsorption of guest molecules, at high temperatures, and at conditions similar to those of catalysis, is unknown and is therefore the subject of the present study. Furthermore, a systematic structural investigation of the cation migration during calcination by two complementary methods, X-ray powder diffraction (XRD) using Rietveld refinement and MAS NMR spectroscopy using spectra-simulation, was carried out for the first time.

Zeolite Y: Framework Structure, Positions of Cations and *m*-Xylene

The structure of zeolite Y is isomorphous with that of the mineral faujasite, as previously determined by X-ray[14,15] and neutron powder diffraction[16] (the space group is $Fd\bar{3}m$ with $a = 24.60$–25.10 Å). The framework is composed of sodalite cages (centred at position 8*a*: 1/8, 1/8, 1/8) linked together in a tetrahedral arrangement by six-membered rings of O(1) atoms to form supercages (centred at position 8*b*: 3/8, 3/8, 3/8).

Extra-framework cation sites were located[17,18] at the following positions (Fig. 1): (i) at the centre of the hexagonal

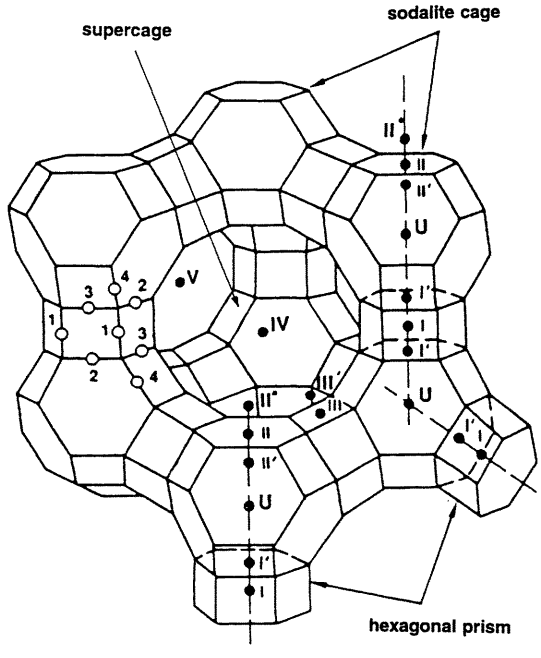

Fig. 1 Structure of zeolite Y (faujasite), the vertices of which are occupied by T atoms (T = Si, Al). The projection is along [111]. The four crystallographic oxygen framework atoms are marked by the numbers 1 to 4. The cation positions are marked by roman numerals (see text).

† Present address: The Royal Institution of Great Britain, Davy Faraday Research Laboratory, 21 Albemarle Street, London, UK W1X 4BS.

View Online

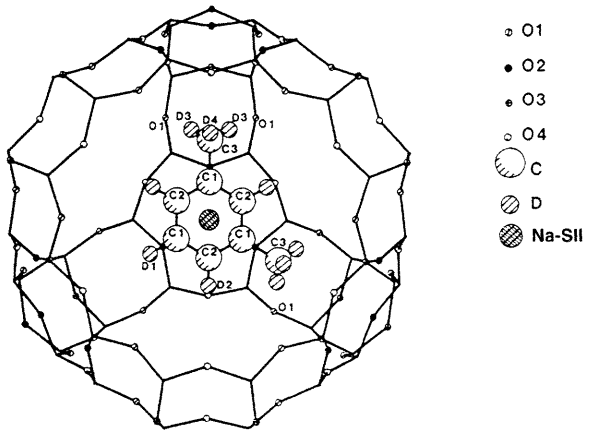

Fig. 2 Location of *m*-xylene in zeolite Y determined by neutron powder diffraction.[19] Only one of six possibilities is shown. The other five are obtained by rotation about the six-fold axis. Silicon is representative for a T atom.

prism [site I (SI)], situated at the origin 3*m* (0, 0, 0), with octahedral coordination to O(3);

(ii) along the three-fold [111] axis for lower-coordinated cations at position 32*e*. Site I′ ($x = y = z \approx 0.06$) inside the sodalite cage enables coordination to three O(3) framework oxygens. Further towards the supercage is site II′ ($x = y = z \approx 0.21$), where coordination to three O(2) oxygens of the six-ring aperture connecting the sodalite to the supercage is obtained. Slightly inside the supercage is site II ($x = y = z \approx 0.23$). Site II* ($x = y = z \approx 0.25$) is shifted to the centre of the supercage. Cations at these two sites are coordinated by three O(2) oxygens of the six-ring window. Special cation positions, often found in hydrated samples, are site IV at the centre of the supercage (position 8*b*, $x = y = z = 3/8$), site V at the centre of the 12-ring window (position 16*d*, $x = y = z = 1/2$) and site U in the centre of the sodalite cage (position 8*a*, $x = y = z = 1/8$);

(iii) at sites III and III′ [position 192*i*, *e.g.* ($x = 0.017$, $y = 0.418$, $z = 0.084$)], near the four-membered rings inside the supercage.

The preferred adsorption site of *m*-xylene[19] is situated in front of the six-ring window, with a distance from the centre of mass to the Na-SII cation, of 2.65 Å (Fig. 2). We denote this position, therefore, as the cation adsorption site. The aromatic plane intersects the [111] axis at right angles.

Experimental

Sample Preparation and Characterization

Zeolite NaY (Bayer AG, Si/Al = 2.34) was thoroughly exchanged with 0.1 mol dm^{-3} $La(NO_3)_3$ solution. The solution was renewed six times and after exchange the zeolite was subsequently washed with decationized water and dried at 323 K. The lanthanum content obtained by EDX (energy dispersive X-ray analysis) represents 73% of the exchange capacity, which corresponds to a composition of $La_{13.9}Na_{15.2}Al_{57}Si_{135}O_{384}$. The calcination was carried out by heating the sample up to the final temperature (given in Table 1) for 24 h at pressures below 10^{-4} mbar. Sample 12 corresponds to sample 11 (*cf.* Table 1) after adsorption of *m*-xylene into the dehydrated zeolite. The dehydrated zeolite LaNaY and *m*-xylene were kept in two different containers within a vacuum-tight glass apparatus at an initial pressure below 10^{-4} mbar at 77 K. The adsorption took place at 298 K over the gas phase initiated by the vapour pressure of *m*-xylene. The coverage was gravimetrically determined and

Table 1 Hydrated and calcined samples of zeolite NaY and the samples of zeolite LaNaY which correspond to the various stages during calcination, prepared for X-ray powder diffraction and MAS NMR spectroscopy

sample no.	zeolite	final temperature of calcination/K
1	NaY	hydrated, rt[a]
2	NaY	623 (24 h)[b]
3	LaNaY-73	hydrated, rt
4	LaNaY-73	323
5	LaNaY-73	363
6	LaNaY-73	393
7	LaNaY-73	423
8	LaNaY-73	473
9	LaNaY-73	543
10	LaNaY-73	623 (0 h)
11	LaNaY-73	623 (24 h)
12	LaNaY-73 (12 *m*-xylene per uc)	623 (24 h)

[a] Room temperature (298 K). [b] Time at the corresponding calcination temperature.

gave *ca.* 12.0 molecules per unit cell (uc). Finally, the samples were enclosed in glass ampoules.

The weight loss of the 50 mg zeolite sample upon heating to 623 K (heating rate of 12.5 K h^{-1}) was determined in a SETARAM TGA 92, 16.18 thermoanalyser under an argon atmosphere. Most of the weight loss, which is due to desorbed water molecules, is observed below 373 K. At higher temperatures, only a small weight loss is obtained (weight is stable at about 523 K). The weight loss of the calcined, in comparison to the hydrated, sample is 24.3 wt.%. Assuming 255 water molecules per uc in the hydrated sample, as determined by Lee and Rees,[4] 236 water molecules per uc are desorbed during calcination, so that about 19 water molecules or OH groups per unit cell remain in the sample calcined at 623 K.

FTIR spectra were recorded on a Perkin Elmer 1750 FTIR spectrometer under a nitrogen atmosphere using the samples of Table 1 additionally loaded with pyridine to detect the Brønsted and Lewis acid sites of the zeolite. The 1543 cm^{-1} band, which is unambiguously attributed to the pyridinium cation[20] and is therefore a probe for the generation of the Brønsted acid sites, was observed only at calcination temperatures higher than 363 K.

X-Ray Diffraction and Refinements

Ex situ X-ray powder diffraction patterns at room temperature were performed with the 12 samples described in Table 1 at a STOE STADIP diffractometer ($4 < 2\Theta/\text{degrees} < 70$ in steps of 0.02°, Ge-monochromatized Cu-Kα_1 radiation, 0.5 mm glass capillaries, 6° PSD).

Ex situ experiments at various temperatures [heating from room temperature (298 K) to 623 K and then cooling in steps of 50 K, recording time for each pattern 1 h] were carried out with the calcined LaNaY (sample 11) at the same diffractometer (40° PSD) using a heating device.

In situ diffractograms of 0.5 g dried zeolite samples were collected on a modified Seifert X-ray diffractometer (Cu-Kα radiation) with a micro-reactor in reflection geometry. The patterns were recorded every 5 h during calcination (10^{-4} mbar, 24 h at 623 K) and at conditions similar to those of catalysis (flow of nitrogen with *m*-xylene was conducted continuously over the calcined zeolite catalyst).

The background of the powder patterns was interpolated by a spline polynomial. The intensities of the background were subtracted from the observed intensities and a mean

Published on 01 January 1995 on http://pubs.rsc.org | doi:10.1039/FT9959101813
Downloaded by Universitat Stuttgart on 20 June 2012

View Online

Published on 01 January 1995 on http://pubs.rsc.org | doi:10.1039/FT9959101813
Downloaded by Universitat Stuttgart on 20 June 2012

background value was added. A straight background was thus obtained. The Rietveld refinements[21] (program RIETAN[22,23]) were based on the framework positions in space group $Fd\bar{3}m$ reported by Fitch *et al.*[16] The first parameters refined were the background, scale factor, zero-shift, asymmetry parameter, profile parameters and the lattice constants (range $4 < 2\Theta/\text{degrees} < 8$ was excluded due to peak asymmetry). Atomic parameters of the zeolite framework were then refined using non-linear constraints for the bond lengths and angles. The guest molecules were located by difference Fourier syntheses using the program FORDAP.[24] Constraints in bond lengths and angles for host and guest were applied and both parts of the structure allowed to vary simultaneously during the last cycles of the Rietveld refinement.

The refinement of hydrated samples with many extra-framework atoms and the possible occupation of two cations (sodium and lanthanum) in one position caused some problems with the Rietveld analysis in this study. These difficulties were solved in the following manner:

(1) The calcined samples were first refined, as the number of extra-framework atoms is small. Furthermore, the atomic positions for these samples are comparable with literature data.[8,16,19]

(2) The sequence of refinements started with the dehydrated sample. Thereafter, patterns were refined in decreasing order of the calcination temperature. The hydrated sample was therefore the last one to be refined. The observed structural changes and the additional extra-framework atoms could be analysed systematically.

(3) An unambiguous assignment of detected extra-framework peaks to sodium, lanthanum, water oxygen or extra-framework aluminium was not achieved. However, sensible results were obtained based on the following criteria: comparison of the coordinates with literature data of cation positions and extra-framework oxygen atoms; comparison of the calculated, based on Rietveld analysis, with the experimentally ($La_{13.9}Na_{15.2}Al_{57}Si_{135}O_{384}$ by EDX) determined composition of the unit cell; calculation of distances to all other atoms of the model zeolite and comparison with typical cation–oxygen, cation–cation, *etc.* distances.

NMR Spectroscopy

For the ^{23}Na and ^{29}Si MAS NMR spectroscopic studies the samples, activated as mentioned above, were introduced into the MAS rotor under a dry-nitrogen atmosphere in a glove box. The ^{27}Al MAS NMR spectra were recorded using fully rehydrated samples. All *ex situ* NMR measurements were carried out at room temperature on a Bruker MSL 400 spectrometer. The spectra were recorded at Larmor frequencies of 105.8 MHz (^{23}Na), 104.3 MHz (^{27}Al) and 79.5 MHz (^{29}Si) with MAS frequencies of 8 kHz (^{23}Na, ^{27}Al) and 3.5 kHz (^{29}Si) using standard double-bearing Bruker MAS probes. Single-pulse excitation corresponding to $\pi/6$ (^{23}Na), $\pi/12$ (^{27}Al) and $\pi/4$ (^{29}Si) was applied. The chemical shifts were referenced to external standards of solid NaCl (^{23}Na), an aqueous solution of $Al(NO_3)_3$ (^{27}Al) and tetramethylsilane (^{29}Si). The MAS NMR spectra were simulated using the PC program WINFIT (Bruker).

Results

X-Ray Diffraction

Ex Situ *X-Ray Diffraction of* LaNaY *during Calcination*

The *R*-values, lattice constants and atomic parameters of selected refined structures of the samples given in Table 1 are listed in Table 2. Some characteristic distances and angles are shown in Table 3.

The Rietveld refinements of the samples given in Table 1 showed distinct changes of the lattice constants of LaNaY during calcination (Fig. 3). After a slight decrease of the lattice constants a continuous increase between 323 and 473 K is observed. *m*-Xylene adsorption leads to an increase in the lattice constants. Pronounced changes in the lattice constants during the calcination of NaY were not observed [24.649 (1) and 24.610 (0) Å for hydrated and calcined NaY, respectively]. The variation of the lattice constants of LaNaY in the course of calcination can, therefore, clearly be assigned to the highly polarising lanthanum cations, which produce a distortion of the TO_4 tetrahedra and hence an alteration of the lattice constant.

Zeolite NaY. No sodium cations were detected at SI, in the hexagonal prism, in either the hydrated or dehydrated sample. The hydrated NaY (sample 1) showed sodium cations at the positions SI′, SII′, SII and SIII. All these positions were also located in the calcined NaY (sample 2) with the exception of SII′. The number of sodium cations at positions SI′ (about 17.2 per uc) and SII (about 15.5 per uc) remains nearly constant after calcination. In sample 1, three extra-framework oxygen atoms detected at positions OW(1), OW(2) and OW(3) are probably associated with water molecules. The oxygen atoms at the positions OW(2) and OW(3) are located in the supercage, whereas OW(1) is in the sodalite cage. All these oxygen atoms are ligands of the sodium cations.

Zeolite LaNaY-73. In the hydrated as-exchanged zeolite LaNaY-73 (sample 3), sodium cations were only found at position SI′ in the sodalite cage. No sodium cations at SI (*cf.* zeolite NaY) were detected in any of the samples 3 to 12. The lanthanum cations are located at the positions SII and SV in the supercage. Rietveld analysis determined a value of 9.8 (0) lanthanum cations per uc for both positions only. This is a deficit of 4.1 (0) lanthanum cations compared with the results obtained by EDX ($La_{13.9}Na_{15.2}Al_{57}Si_{135}O_{384}$, see Experimental). These 4.1 (0) non-localized lanthanum cations are presumably lanthanum cations, which are distributed over the whole supercage. Three extra-framework oxygen atoms were located at the positions OW(1), OW(2) and OW(3).

Fig. 4 displays the occupation of cation positions by lanthanum and sodium cations after calcination at increasing temperatures. In addition, the population of the extra-framework

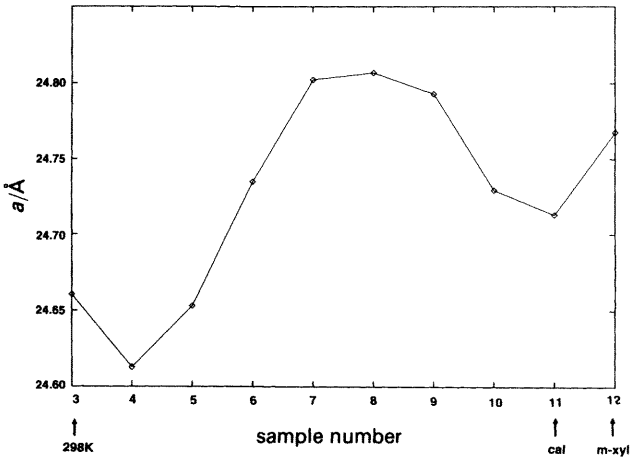

Fig. 3 Changes of the lattice constant *a* of zeolite LaNaY-73 during calcination. The hydrated sample is marked by 298 K, the calcined sample (24 h at 623 K) by cal, and the sample loaded with *m*-xylene by *m*-xyl. The error bars are smaller than the symbols of the lattice constants.

View Online

Table 2 Atomic parameters, lattice constants and *R*-values resulting from the Rietveld refinement of selected LaNaY samples in space group $Fd\bar{3}m$

			zeolite LaNaY sample[a]			
atom	position	atomic parameter	3	8	11	12
T = Si, Al	192*i*	*x*	−0.054 (7)	−0.053 (3)	−0.056 (3)	−0.053 (1)
		y	0.536 (0)	0.534 (9)	0.534 (5)	0.535 (9)
		z	0.630 (4)	0.625 (3)	0.625 (3)	0.625 (5)
		occ[b]	192	192	192	192
		B_{iso}[c]	1.5	1.5	1.5	1.5
O(1)	96h	*x*	−0.108 (2)	−0.106 (7)	−0.108 (1)	−0.106 (8)
		y = 1/2				
		z	0.608 (2)	0.606 (7)	0.608 (1)	0.606 (8)
		occ	96	96	96	96
		B_{iso}	2.0	2.0	2.0	2.0
O(2)[d]	96*g*	*x*	−0.003 (2)	−0.002 (3)	−0.004 (1)	−0.002 (6)
		y = *x* + 1/2				
		z	0.649 (2)	0.639 (2)	0.640 (6)	0.640 (9)
		occ	96	96	96	96
		B_{iso}	2.0	2.0	2.0	2.0
O(3)	96*g*	*x*	−0.029 (1)	−0.033 (8)	−0.035 (8)	−0.032 (5)
		y = *z*	0.580 (4)	0.575 (7)	0.574 (0)	0.574 (8)
		occ	96	96	96	96
		B_{iso}	2.0	2.0	2.0	2.0
O(4)	96*g*	*x*	−0.071 (0)	−0.069 (3)	−0.068 (8)	−0.068 (8)
		y	0.569 (2)	0.572 (9)	0.571 (2)	0.571 (2)
		z = 5/4 − *y*				
		occ	96	96	96	96
		B_{iso}	2.0	2.0	2.0	2.0
Na(SI′)	32*e*	*x* = *y* = *z*	0.079 (1)	—	—	—
		occ	14.0 (4)	—	—	—
		B_{iso}	4.0			
Na(SII)	32*e*	*x* = *y* = *z*	—	0.234 (0)	0.236 (1)	0.236 (8)
		occ	—	12.0 (9)	9.0 (6)	16.0 (2)
		B_{iso}	—	4.0	4.0	4.0
La(SI′)	32*e*	*x* = *y* = *z*	—	0.067 (2)	0.065 (2)	0.066 (8)
		occ	—	14.0 (6)	14.0 (2)	13.0 (2)
		B_{iso}	—	3.0	3.0	3.0
La(SII)	32*e*	*x* = *y* = *z*	0.246 (8)	—	—	—
		occ	4.9 (0)	—	—	—
		B_{iso}	3.0	—	—	—
La(SV)	16*d*	*x* = *y* = *z*	0.5	—	—	—
		occ	4.9 (0)	—	—	—
		B_{iso}	3.0	—	—	—
OW(1)	96*g*	*x* = *z*	0.089 (7)	0.085 (8)	0.077 (8)	0.078 (3)
		y	0.192 (7)	0.164 (3)	0.152 (1)	0.155 (7)
		occ	59.0 (5)	24.0 (5)	42.0 (2)	20.0 (1)
		B_{iso}	8.0	8.0	8.0	8.0
OW(2)	192*i*	*x*	0.034 (2)	—	—	—
		y	0.493 (5)	—	—	—
		z	0.173 (3)	—	—	—
		occ	69.0 (5)	—	—	—
		B_{iso}	8.0	—	—	—
OW(3)	192*i*	*x*	0.530 (2)	—	—	—
		y	0.430 (7)	—	—	—
		z	0.420 (3)	—	—	—
		occ	26.0 (8)	—	—	—
		B_{iso}	8.0	—	—	—
C(1)	96*g*	*x* = *z*	—	—	—	0.270 (6)
		y	—	—	—	0.366 (6)
		occ	—	—	—	30.0 (5)
		B_{iso}	—	—	—	8.0
C(2)	96*g*	*x* = *z*	—	—	—	0.321 (7)
		y	—	—	—	0.266 (5)
		occ	—	—	—	30.0 (5)
		B_{iso}	—	—	—	8.0
C(3)	96*g*	*x* = *z*	—	—	—	0.347 (2)
		y	—	—	—	0.212 (8)
		occ	—	—	—	20.0 (3)
		B_{iso}	—	—	—	8.0

Published on 01 January 1995 on http://pubs.rsc.org | doi:10.1039/FT9959101813
Downloaded by Universitat Stuttgart on 20 June 2012

View Online

Table 2 Continued

		zeolite LaNaY sample[a]			
		3	8	11	12
lattice constants/Å	$a = b = c$	24.660 (6)	24.806 (8)	24.713 (5)	24.767 (6)
R-values	R_p	3.43	1.76	2.59	1.81
	R_{wp}	4.73	2.25	3.50	2.38

[a] See Table 1 for sample numbering. [b] occ: occupation in atoms (ions) per unit cell. [c] B_{iso}: isotropic temperature factor. [d] The simplest equivalent position for atoms in 96*g* is *x*, *x*, *z*. However, in order to give the coordinates for the oxygen atoms O(1) to O(4) bonded to the same Si atom, we have chosen other (more complicated) symmetry equivalents for atoms O(2) to O(4).

oxygen atoms at position OW(1) is depicted. After calcination at 393 K (sample 6), a distinct change in these occupation numbers is observed. Lanthanum migrates from the supercage into the sodalite cage [Fig. 4(*a*)], so that all lanthanum ions [14.0 (2) ions per uc] are located at position SI′ in the calcined sample. This migration process is approximately completed at 473 K. The lanthanum population of position SV vanishes at temperatures above 363 K (sample 5), whereas low occupation of the position SII by lanthanum [1.0 (0) and 0.0 (7) ions per uc, respectively] is obtained at temperatures of 393 and 423 K.

A migration of the sodium cations in the opposite direction to that of the lanthanum cations from sodalite cage to supercage was detected [Fig. 4(*b*)]. After calcination at temperatures higher than 393 K, only sodium cations located on SII are observed. The population of this position, however, varies with increasing calcination temperature between 9.0 (6) and 15.0 (5) sodium cations per uc. The maximum is reached at 543 K (sample 9). In this sample all sodium cations are located at position SII. After calcination above 543 K (samples 10 and 11) a decrease of the SII population is obtained, so that only 9.0 (6) (sample 11) of the 15.2 (15.2 per uc was obtained by EDX, see Experimental) sodium cations per uc are situated at this position.

Only one extra-framework oxygen atom, probably a water oxygen atom, was localized at position OW(1) in the sodalite cage above 363 K. This extra-framework oxygen atom is a ligand to the La SI′ [3.0 (0) and 1.0 (3) extra-framework oxygen atoms coordinate to one lanthanum cation at position SI′ at 393 and 543 K, respectively]. Up to a calcination temperature of 543 K, an expected decrease of the population

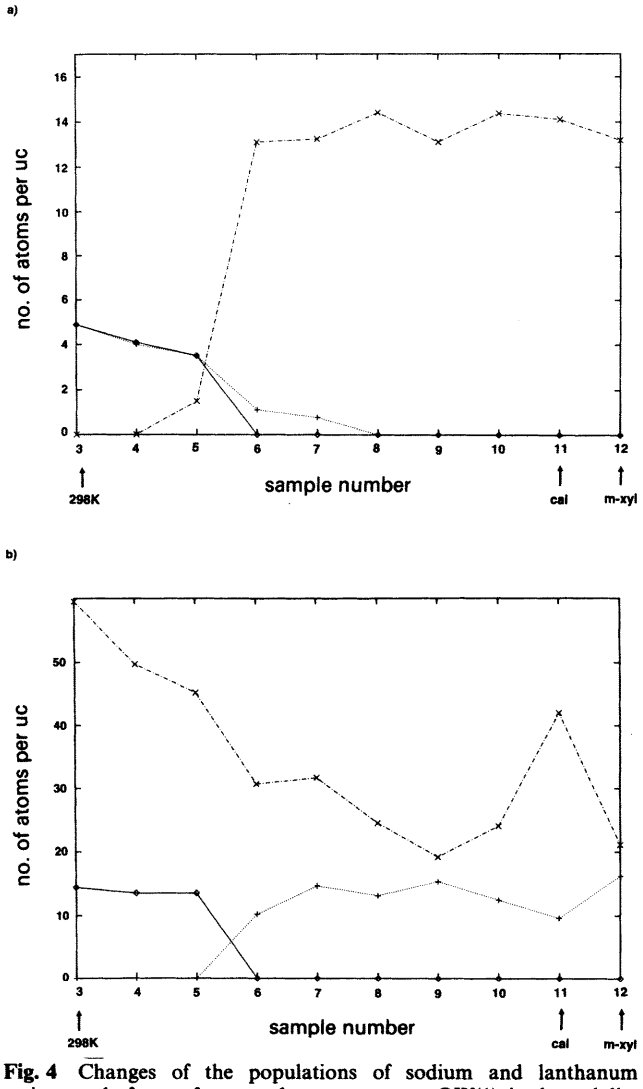

Fig. 4 Changes of the populations of sodium and lanthanum cations and of extra-framework oxygen atoms, OW(1), in the sodalite cage with increasing calcination. The hydrated sample is marked by 298 K, the calcined sample (24 h at 623 K) by cal, and the sample loaded with *m*-xylene by *m*-xyl. (*a*) Population of lanthanum positions: La-SV (◇), La-SII (+) and La-SI′ (×). (*b*) Population of sodium and oxygen positions: Na-SI′ (◇), Na-SII (+) and OW(1) (×).

Table 3 Selected distances (Å) and angles (degrees) between the framework atoms, sodium and lanthanum, extra-framework oxygen and the carbon of *m*-xylene

	zeolite NaY sample[a]			
	3	8	11	12
		framework		
T–O(1)	1.68 (2)	1.65 (4)	1.60 (6)	1.65 (3)
T–O(2)	1.66 (1)	1.61 (4)	1.64 (3)	1.62 (8)
T–O(3)	1.73 (4)	1.68 (0)	1.69 (3)	1.67 (1)
T–O(4)	1.56 (2)	1.64 (5)	1.63 (0)	1.64 (5)
mean T–O	1.65 (9)	1.64 (8)	1.64 (3)	1.64 (9)
O(1)–T–O(2)	112.5 (2)	112.9 (2)	112.2 (8)	111.5 (8)
O(1)–T–O(3)	112.3 (7)	110.4 (6)	109.6 (5)	110.1 (6)
O(1)–T–O(4)	109.8 (6)	109.1 (7)	110.8 (7)	108.7 (4)
O(2)–T–O(3)	106.3 (6)	106.1 (5)	105.4 (4)	106.4 (6)
O(2)–T–O(4)	106.5 (7)	110.6 (8)	105.5 (0)	108.1 (2)
O(3)–T–O(4)	109.0 (5)	107.4 (7)	113.0 (1)	111.8 (5)
mean O–T–O	109.4 (5)	109.4 (7)	109.3 (7)	109.4 (8)
T–O(1)–T	142.1 (3)	136.5 (8)	136.5 (9)	136.8 (1)
T–O(2)–T	144.2 (0)	149.7 (0)	149.7 (0)	148.8 (4)
T–O(3)–T	137.5 (0)	144.2 (3)	141.9 (4)	141.3 (4)
T–O(4)–T	142.1 (0)	147.1 (8)	145.9 (8)	144.3 (1)
mean T–O–T	141.8 (8)	144.2 (2)	143.5 (5)	142.8 (3)
		extra-framework		
M[b](SI′)–O(3) (3×)	2.66 (2)	2.52 (8)	2.51 (7)	2.47 (4)
M(SI′)–OW(1) (3×)	2.09 (7)	2.45 (4)	2.11 (9)	2.28 (6)
M(SII)–O(2) (3×)	2.41 (6)	2.44 (0)	2.44 (0)	2.44 (0)
M(SII)–C(X)[c] (3×)	—	—	—	3.06 (5)

[a] See Table 1. [b] M: sodium or lanthanum (see Table 2) at cation site in parentheses. [c] C: shortest C(X)–M(SII) distance.

Published on 01 January 1995 on http://pubs.rsc.org | doi:10.1039/FT9959101813
Downloaded by Universitat Stuttgart on 20 June 2012

View Online

Published on 01 January 1995 on http://pubs.rsc.org | doi:10.1039/FT9959101813
Downloaded by Universitat Stuttgart on 20 June 2012

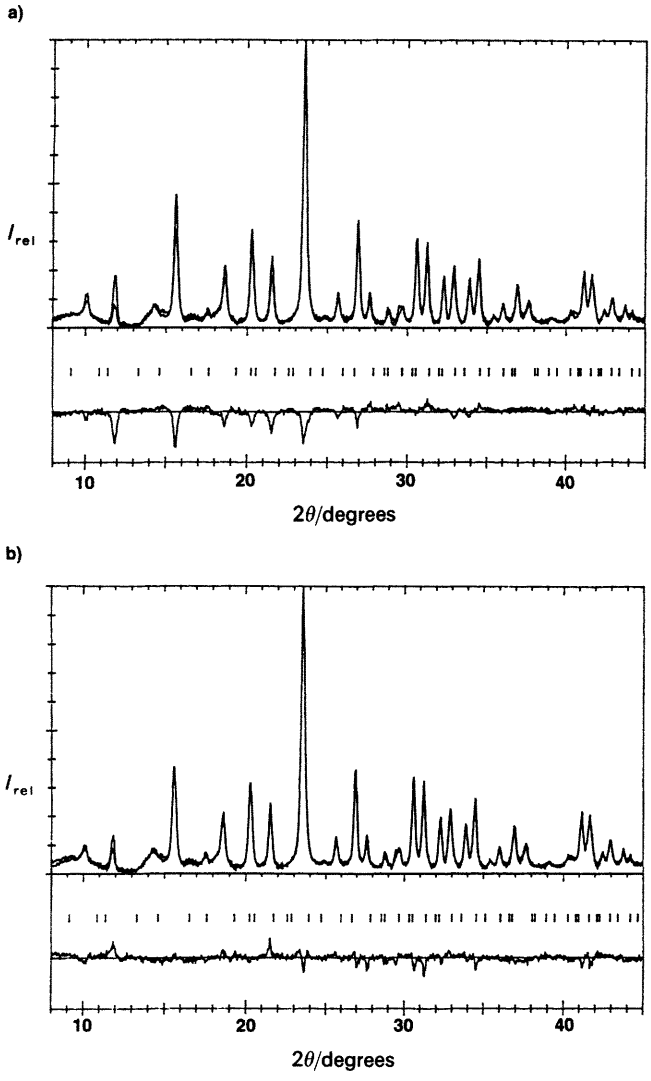

Fig. 5 Difference diagrams (bottom) of the X-ray powder patterns of LaNaY-73 recorded at 298 and 623 K. The superpositions of the observed X-ray powder patterns are shown as solid lines (top). (*a*) Difference diagram on heating. (*b*) Difference diagram of both 298 K diffractograms before heating and after cooling.

of this position was determined [Fig. 4(*b*)]. Further calcination, however, shows a surprising result: an increase of the occupation number of the OW(1) oxygen atom. Rietveld analysis yielded too many extra-framework oxygen atoms [42.0 (2) atoms per uc] in comparison with the residual water content (19 molecules per uc; see Experimental) obtained by thermogravimetric experiments. The refinements showed that this population number has a minor influence on the quality of the refinement, so that the value of 42.2 atoms per uc determined by Rietveld analysis is only a rough estimate. This result, however, clearly indicates an increase of the electron density in the sodalite cage around the OW(1) position which is hardly explained by the increase of 23 oxygen atoms at this position. High static disorder can therefore be proposed for the atoms located at position SI′. This is additionally supported by the high isotropic temperature factor (*cf.* Table 2).

There are several explanations for the increase of the electron density at the OW(1) position. We assume that sodium cations migrate at temperatures above 543 K from supercage to sodalite cage. This assumption is based on a relationship between the population of the sodium cations located on position SII and oxygen atoms located on OW(1) for samples 9 to 11: the increase of the OW(1) population corresponds to the decrease of the sodium SII population. This sodium position was not previously described as a cation position in faujasite-type zeolites. This observation is further supported by (i) the structure refinement of the calcined sample after adsorption of *m*-xylene, (ii) the temperature-dependent *ex situ* X-ray diffraction and (iii) the *in situ* diffraction experiments (see below). All these experiments showed a relationship between sodium cations at position SII and oxygen atoms at position OW(1). In particular, the data of the adsorbed samples [20.0 (1) oxygen atoms per uc at position OW(1) and 16.0 (2) sodium cations per uc at site II] give strong support to our assumption. Dealumination might be a second reason for the increase of the electron density in the sodalite cage. The decrease of the lattice constant above 473 K (*cf.* Fig. 3) indicates this.[25]

m-Xylene was located at the cation adsorption site, in front of the six-ring window (*cf.* Fig. 2), in good agreement with experimental[19] and theoretical investigations.[26] Adsorption of *m*-xylene causes a guest-molecule-induced sodium migration, probably from the sodalite cage (*cf.* results in last paragraph) to position SII in the supercage [*cf.* Fig. 4(*b*)]. All sodium cations [16.0 (2) cations per uc] occupy position SII after guest-molecule loading. Only oxygen atoms [20.0 (1) per uc by XRD, 19.0 per uc by thermogravimetry (TG)] are located at position OW(1). Lanthanum ions are not influenced by guest-molecule adsorption.

Temperature-dependent ex situ *X-Ray Diffraction of the Calcined* LaNaY

A sequence of X-ray powder patterns of sample 11 were recorded on heating from 298 to 623 K and then cooling from 623 to 298 K. Reversible changes of the intensities are observed, especially at low 2θ values. The difference of the diffractograms recorded at 298 and 623 K after heating [Fig. 5(*a*)] shows distinct changes of the intensities and indicates structural alterations on heating. Strong evidence for the reversibility of these structural alterations is given in Fig. 5(*b*), where the difference diagram of both 298 K powder patterns (before heating and after cooling) is shown. Only minor differences in the intensities are observed.

Rietveld refinements were carried out to quantify these observations. The Rietveld difference plots are shown in Fig. 6. The room-temperature structure is identical to that of the refined calcined LaNaY (sample 11) described above. Heating at 623 K results in an increase of the SII population of 6.0 (2) sodium cations per uc [from 9.0 (6) to 15.0 (8) ions per uc] and a correlated decrease of the OW(1) population (*cf. ex situ* XRD of LaNaY during calcination). This is strong evidence for a temperature-induced sodium migration from the sodalite cage to position SII in the supercage. In the high-temperature structure all sodium cations are located on position SII. The lanthanum cations at SI′ in the sodalite cage are not influenced by heating.

In situ *X-Ray Diffraction of* LaNaY

The X-ray powder patterns of LaNaY-73 recorded during calcination and at conditions similar to those of catalysis are shown in Fig. 7. The pronounced changes of the intensities during the calcination from 298 to 623 K [Fig. 7(*a*)] are due to cation migration (lanthanum from supercage to sodalite cage, sodium migration from sodalite cage to supercage). Upon exposing the calcined zeolite to a stream of *m*-xylene–N_2 at a temperature of 623 K for up to 100 h, however, only small alterations in the intensities of the X-ray powder patterns were observed. Rietveld analysis of two X-ray powder patterns (calcined sample and sample after 20 h on stream of *m*-xylene–N_2) yielded good agreement with

View Online

Published on 01 January 1995 on http://pubs.rsc.org | doi:10.1039/FT9959101813
Downloaded by Universitat Stuttgart on 20 June 2012

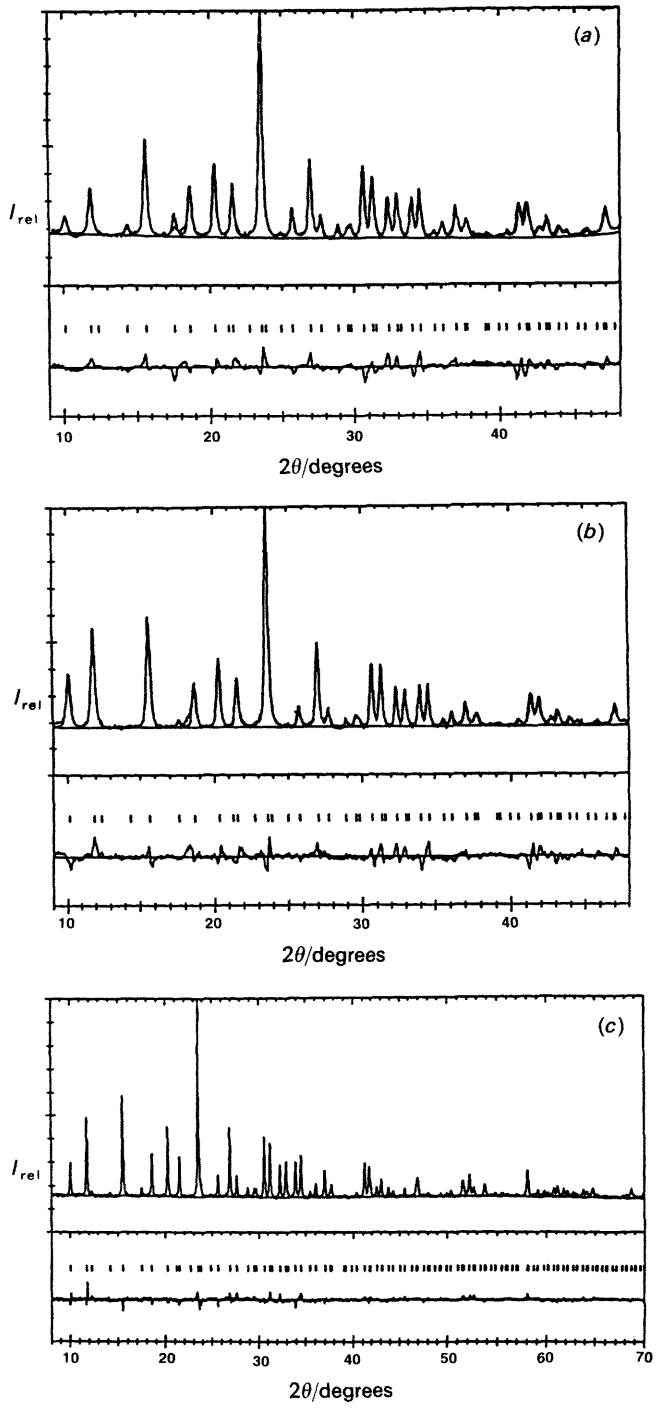

Fig. 6 Observed, calculated and difference profiles for the Rietveld refinement of the temperature-dependent *ex situ* X-ray powder patterns of dehydrated (24 h at 623 K) LaNaY-73 at 298 K (*a*) and 623 K (*b*) recorded with a 40° PSD. (*c*) Corresponding refinement of the *ex situ* XRD experiments during calcination for the same sample at 298 K recorded with 6° PSD, shown for comparison.

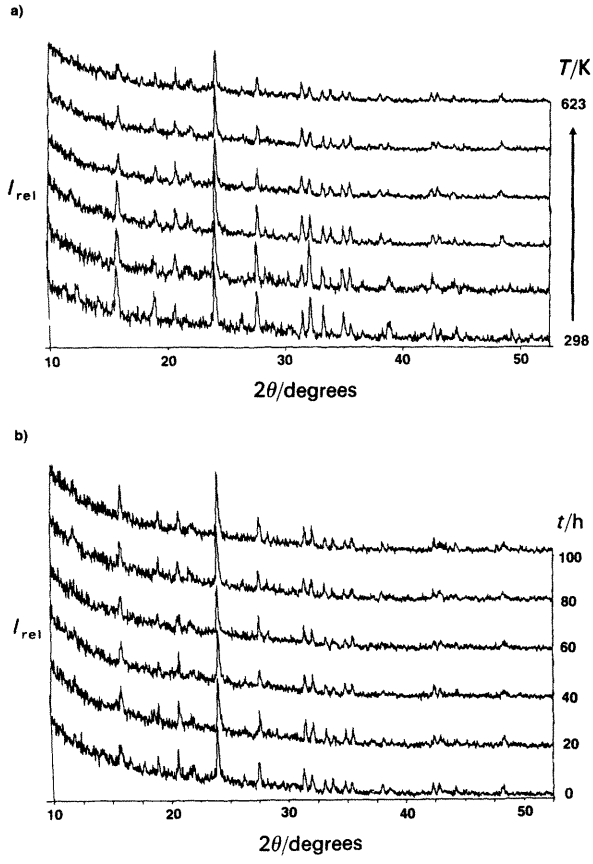

Fig. 7 *In situ* X-ray powder patterns of zeolite LaNaY-73 during calcination from 298 to 623 K (*a*) and of the calcined sample under a stream of *m*-xylene–N_2 at 623 K for times up to 100 h (*b*)

the *ex situ* diffraction experiments. Hence the zeolite structure model obtained from *ex situ* measurements describes the zeolite framework and the population of the cation sites at catalytic conditions sufficiently well.

The structure of the calcined sample is identical to the high-temperature structure (623 K) obtained by *ex situ* X-ray powder diffraction experiments (see above). All lanthanum cations are located at position SI′ in the sodalite cage in the calcined sample and in the sample during catalysis. The lanthanum cations are coordinated to three O(2) framework oxygens and 1.0 (2) water oxygen atoms at position OW(1). The population of sodium cations at SII was 16.0 (0) per uc, so that all sodium cations are localized at this position.

Rietveld refinement of the sample at conditions similar to those of catalysis yielded virtually unmodified framework positions. Furthermore, all lanthanum cations are at position SI′, coordinated to three O(2) and 1.0 (1) water oxygen atoms at position OW(1). The refinement yielded an occupation of 26.0 (1) sodium cations per uc at position SII. Fourier analysis of the powder pattern revealed residual electron density at the cation adsorption site and led to the inclusion of *m*-xylene in the Rietveld refinement. Distinctly improved *R*-values and sensible population numbers for the guest molecule atoms (16 molecules per uc) provide strong evidence for the presence of the guest molecule at the preferred adsorption site (cation adsorption site, *cf.* Fig. 2). However, the population of sodium [26.0 (1) Na^+ per uc] is too high (about 10 sodium cations per uc) compared with the sodium content obtained by EDX (15.2 Na^+ per uc, *cf.* Experimental) and the population of the calcined (*in situ*) sample [16.0 (0)]. The difference might be explained by additional electron density in the region of the six-ring window, which originates from adsorbed guest molecules. The aromatic guest molecules should be closer to the zeolite wall, if the sodium SII position is empty (only 16 of the 32 cation sites per uc are occupied). However, a second guest molecule was not located by difference Fourier analysis. Also, a refinement including a *m*-xylene molecule close to the six-ring window was not successful. Therefore, we interpreted these results as being due to high static disorder of the aromatic guest molecules at six-ring windows with an empty sodium site.

View Online

Published on 01 January 1995 on http://pubs.rsc.org | doi:10.1039/FT9959101813
Downloaded by Universitat Stuttgart on 20 June 2012

MAS NMR Spectroscopy

^{29}Si *MAS NMR Spectroscopy*

The ^{29}Si MAS NMR spectra of the hydrated parent zeolite NaY (sample 1) and the hydrated as-exchanged zeolite LaNaY-73 (sample 3) depicted in Fig. 8(*a*) and (*b*), respectively, consist of lines at the following chemical shifts: −83.5, −89.2, −94.5, −100.5 and −105.0 ppm. From the intensities of these lines, which are caused by framework silicon atoms [Si(*n*Al) with $n = 4$, 3, 2, 1 and 0 (see bottom of each spectrum)], framework, n_{Si}/n_{Al} ratios of 2.4 and 2.5 for zeolites NaY and LaNaY, respectively, were calculated.[27]

After dehydration of zeolite LaNaY, a decrease in the intensities of the Si(4Al), Si(3Al) and S(2Al) lines can be observed which is coupled with the appearance of a new peak at about −97 ppm. Recent solid-state NMR studies[5] on homologous series of lanthanum-exchanged zeolites Y have verified quantitatively the suggestion of Chao and Chern[28] that the migration of lanthanum cations into the sodalite cages causes a strain of Si—O—T bonds in the six-ring window (sw) close to La^{3+} at position SI′. In the ^{29}Si MAS NMR spectra of dehydrated zeolite LaNaY, this local framework strain is responsible for a shift in the resonance position of the corresponding silicon atoms by about 3 ppm to higher magnetic field.[5,11] Therefore, the simulation of the ^{29}Si MAS NMR spectra of zeolite LaNaY dehydrated for 24 h at 623 K before [Fig. 8(*c*)] and after [Fig. 8(*d*)] adsorption of *m*-xylene was carried out by assuming additional lines 3′, 2′ and 1′ (lines shifted by about 3 ppm). Because of the small intensity of the Si(4Al) signal in Fig. 8(*a*) and (*b*), this line was neglected in Fig. 8(*c*) and (*d*). The decomposition of the ^{29}Si MAS NMR spectra in Fig. 8(*c*) and (*d*) into two sets of Si(*n*Al) and Si(*n*′Al) signals reveals that in both samples, before and after adsorption of *m*-xylene, 40(±5)% of the framework silicon atoms contribute to strained Si—O—T bonds.

The framework composition of the actual zeolite Y (57 Al per uc and 135 Si per uc) corresponds to a mean number of

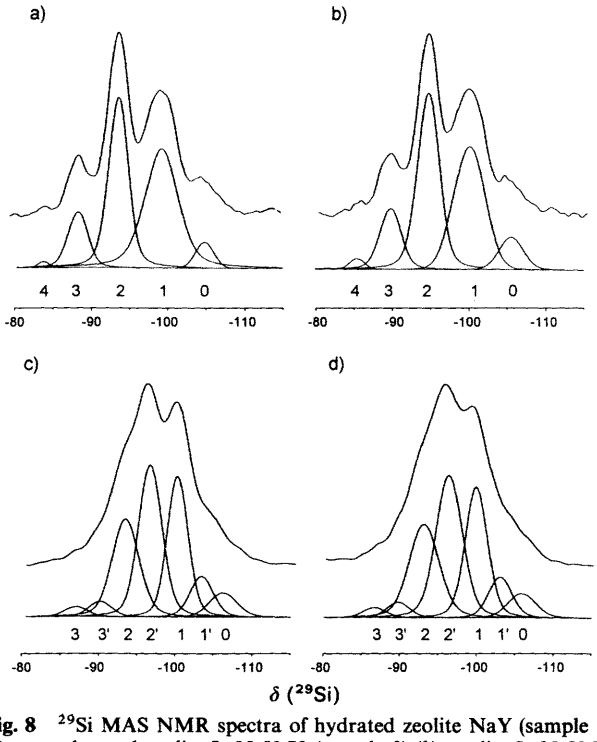

Fig. 8 ^{29}Si MAS NMR spectra of hydrated zeolite NaY (sample 1) (*a*), as-exchanged zeolite LaNaY-73 (sample 3) (*b*), zeolite LaNaY-73 dehydrated for 24 h at 623 K (sample 11) (*c*) and LaNaY-73 dehydrated at 623 K and loaded with *m*-xylene (sample 12) (*d*)

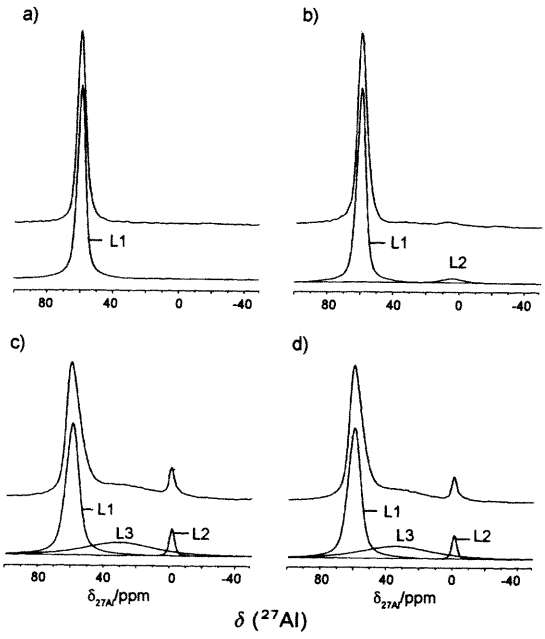

Fig. 9 ^{27}Al MAS NMR spectra of hydrated zeolite LaNaY-73 (sample 1) (*a*), as-exchanged zeolite LaNaY-73 (sample 3) (*b*), zeolite LaNaY-73 calcined for 24 h at 623 K and rehydrated (sample 11) (*c*), and zeolite LaNaY-73 calcined at 623 K and loaded with *m*-xylene and rehydrated (sample 12) (*d*)

4.3 silicon atoms per sw and 1.7 aluminium atoms per sw. Hence a strain of about 40% of all Si—O—T bonds corresponds to 12.6 strained six-ring windows per unit cell [(0.4 × 135 Si per uc)/4.3 Si per sw]. The value of 12.6 La^{3+} per uc located on SI′ determined by ^{29}Si MAS NMR spectroscopy is in reasonable agreement with the total number of 13.9 lanthanum cations per uc. Considering the accuracy of the line decomposition, we can conclude that all lanthanum cations in sample 11 as well as in sample 12 are located in the sodalite cages at position SI′. The adsorption of *m*-xylene onto dehydrated zeolite LaNaY, therefore, does not affect the local structure of lanthanum cations.

^{27}Al *MAS NMR Spectroscopy*

Fig. 9 shows the ^{27}Al MAS NMR spectra of the samples 1, 3, 11 and 12. Before the measurements, the calcined samples 11 and 12 were rehydrated. While the spectrum of the parent zeolite NaY [Fig. 9(*a*)] consists only of the signal of tetrahedrally coordinated framework aluminium at a chemical shift of 60 ppm (L1), the spectrum of the as-exchanged zeolite LaNaY [Fig. 9(*b*)] shows an additional weak signal of extra-framework aluminium at about 0 ppm (L2). As shown in Fig. 9(*c*), the calcination of zeolite LaNaY at 623 K causes an increase in the extra-framework aluminium signal (L2) of up to 5% of the total ^{27}Al MAS NMR intensity. This corresponds to an increase of the framework n_{Si}/n_{Al} ratio from 2.5 to 2.6. In addition, a broad signal (L3) appears at a chemical shift of about 35 ppm with a linewidth of about 50 ppm. Application of the double rotation (DOR) NMR technique (not shown) did not result in a narrowing of signal L3. The decomposition of the spectrum in Fig. 9(*c*) yields an intensity of this signal of 35(±5)%. Solid-state NMR studies[5] of a homologous series of lanthanum-exchanged zeolites Y, produced a shift of the signal L3 at 35 ppm with increasing extent of lanthanum exchange in parallel with the high-field shifted ^{29}Si MAS NMR signals, Si(*n*′Al), of the framework silicon atoms. The authors conclude, therefore, that these observations have a common origin. Lanthanum migration to position SI′ in the sodalite cages strains the Si—O—T and

View Online

Published on 01 January 1995 on http://pubs.rsc.org | doi:10.1039/FT9959101813
Downloaded by Universitat Stuttgart on 20 June 2012

Al—O—T bonds. The local framework strain of the Al—O—T bonds causes an increase in the quadrupole coupling constant of the corresponding aluminium atoms[29] and a high-field shift originating from the second-order quadrupole interaction of these ^{27}Al nuclei. Since the application of the DOR technique does not narrow the spectrum, the linewidth of the signal at 35 ppm is due to a distribution of quadrupole parameters or chemical shifts.

Upon comparing the ^{27}Al MAS NMR spectra of the rehydrated zeolite LaNaY activated 24 h at 623 K before [Fig. 9(*c*)] and after [Fig. 9(*d*)] adsorption of *m*-xylene, no change in the lineshapes and intensities can be observed. This is in agreement with the above-mentioned results of ^{29}Si MAS NMR spectroscopy and indicates that the guest molecule, *m*-xylene, has no influence on the location of lanthanum cations and the local framework strain in zeolite LaNaY.

^{23}Na *MAS NMR Spectroscopy*

In Fig. 10, the ^{23}Na MAS NMR spectra of hydrated and dehydrated zeolites NaY and LaNaY-73 are depicted. The spectra of the hydrated zeolite NaY [Fig. 10(*a*)] and the as-exchanged zeolite LaNaY [Fig. 10(*c*)] consist of two signals at −9 ppm (L1) and −13 ppm (L2). While the former signal was assigned to extra-framework sodium cations in the large cavities, the latter was attributed to sodium cations in the sodalite cages.[5,11,30–32] In contrast to signal L1, which is not affected by quadrupolar interactions in the ^{23}Na MAS NMR spectrum of the as-exchanged zeolite LaNaY, an additional signal, L3, at about −14 ppm was observed which shows a second-order quadrupolar shift corresponding to a quadrupole coupling constant of 0.7 ± 0.1 MHz.[5] Therefore, the determination of the numbers of sodium cations requires a correction of the experimentally observed relative ^{23}Na MAS NMR intensities, I_{obs}, using the method proposed by Massiot *et al.*[33] (see also ref. 5 and ref. 34). Columns 4 and 5 of Table 4 give a summary of the numbers of sodium cations in the large cavities (L1) and sodalite cages (L2 or L3), respectively, of samples 1 and 3, calculated using the total number of sodium cations (EDX) and the corrected relative ^{23}Na MAS NMR intensities. Considering these figures, an exchange of 73% of sodium cations in zeolite NaY by lanthanum cations results in a decrease in the number of sodium cations in the large cavities from 27.0 Na^+ per uc to 1.7 Na^+ per uc and in the sodalite cages from 29.3 Na^+ per uc to 13.5 Na^+ per uc. Hence, in the large cavities of the as-exchanged zeolite LaNaY almost all sodium cations were replaced by lanthanum cations. The residual sodium cations of the as-exchanged zeolite LaNaY are mainly located in the sodalite cages.

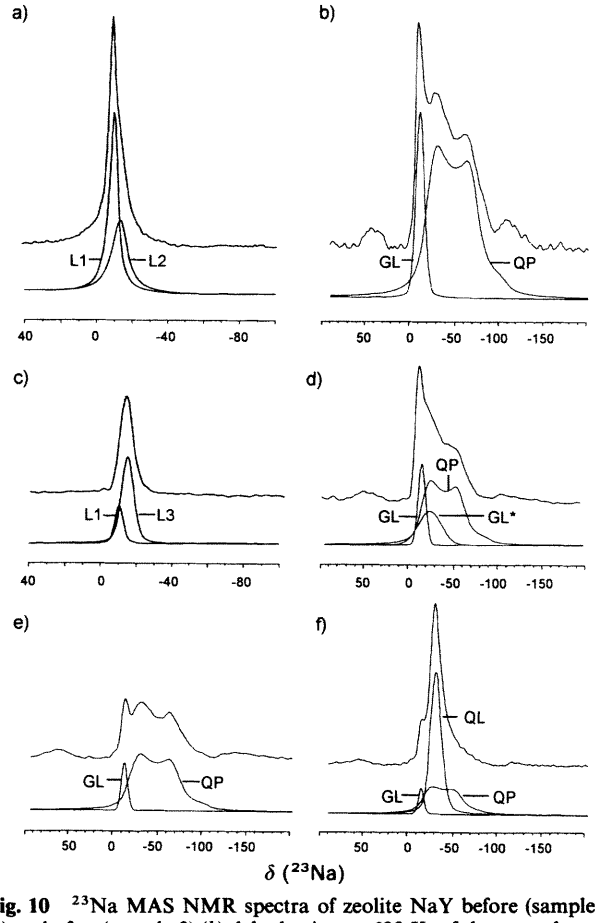

Fig. 10 ^{23}Na MAS NMR spectra of zeolite NaY before (sample 1) (*a*) and after (sample 2) (*b*) dehydration at 623 K, of the as-exchanged zeolite LaNaY-73 (sample 3) (*c*), zeolite LaNaY-73 dehydrated at 473 K (sample 8) (*d*), dehydrated for 24 h at 623 K (sample 11) (*e*), and dehydrated zeolite LaNaY-73 (24 h at 623 K) loaded with *m*-xylene (sample 12) (*f*)

Table 4 Experimentally observed relative ^{23}Na MAS NMR intensities (I_{obs}) of the signals L1, L2 and L3 of hydrated zeolites NaY and LaNaY-73 [see Fig. 10(*a*) and (*c*)], the number of sodium cations (n_i) per unit cell calculated from the corrected intensities, I_{obs},[a] and the total number of sodium cations determined by EDX (NaY, 56.3 Na^+ per uc, LaNaY, 15.2 Na^+ per uc)

hydrated samples	I_{obs} (%)		n_{L1} (in large cavities)	n_{L2}, n_{L3} (in sodalite cage)
	$L1_{obs}$	$L2_{obs}$, $L3_{obs}$		
1	48	52	27.0	29.3
3	22	78	1.7	13.5

[a] Correction method proposed by Massiot *et al.*[33]

The spectra of dehydrated Y-type zeolites in Fig. 10(*b*) and (*e*) consist of two components, a low-field Gaussian line (GL) of the sodium cations located at position SI at a chemical shift of −13 ppm and a high-field quadrupolar pattern (QP) of sodium cations located on positions SI′ and SII which shows singularities at about −31 ppm and −63 ppm.[34] The quadrupole coupling constant (χ) of the sodium cations of these signals are *ca.* 100 kHz and 4.2 MHz,[34] respectively. Recent ^{23}Na MAS NMR investigations of dehydrated zeolite NaY at magnetic field strengths of $B_0 = 9.4$ T ($\nu_0 = 105.8$ MHz) and 17.6 T ($\nu_0 = 198.4$ MHz)[35] showed that the QP signal can be decomposed into two patterns, a pattern of Na^+ located at SII with a χ value of 4.0 MHz and a pattern of Na^+ located at SI′ with a χ value of 4.8 MHz. However, the ^{23}Na MAS NMR spectra of dehydrated zeolites NaY and LaNaY recorded only at one resonance frequency renders a reliable decomposition of the QP signal into two patterns difficult.

Columns 5 and 7 of Table 5 give the numbers of sodium cations located at position SI (signal GL) and on positions SI′ and SII (signal QP), respectively. As mentioned above, these figures were calculated using the corrected relative ^{23}Na MAS NMR intensities and the total number of sodium cations determined by EDX. Considering these figures, after lanthanum exchange of zeolite NaY the sodium population of position SI of dehydrated samples decreases from 2.6 Na^+ per uc. The number of sodium cations responsible for signal QP decreases from 53.7 Na^+ per uc to 14.9 Na^+ per uc.

The decomposition of the spectrum of zeolite LaNaY activated at 473 K [Fig. 10(*d*)] requires the assumption of a second Gaussian line (GL*) at a chemical shift of −24 ppm. Since this signal was also observed in partially rehydrated

View Online

Table 5 Experimentally observed relative ^{23}Na MAS NMR intensities (I_{obs}) of the signals GL, GL* and QP of the dehydrated zeolites NaY and LaNaY-73 [see Fig. 10(*b*), (*d*), (*e*) and (*f*)], the number of sodium cations (n_i) per unit cell calculated from the corrected intensities, I_{obs},[a] and the total number of sodium cations determined by EDX (NaY, 56.3 Na^+ per uc; LaNaY, 15.2 Na^+ per uc)

	I_{obs} (%)					
dehydrated samples	GL_{obs}	GL^*_{obs} or QL_{obs}	QP_{obs}	n_{GL} (at SI)	n_{GL^*} or n_{QL} (interacting with guests)	n_{QP} (at SI′ and at SII)
2	23		77	2.6		53.7
8	14	21	65	0.5	0.9	13.8
11	10		90	0.3		14.9
12	4	72	24	0.4	9.1	5.7

[a] Correction method proposed by Massiot *et al.*[33]

zeolites NaY,[5] the line GL* was attributed to sodium cations interacting with at least one water molecule. As depicted in Fig. 10(*f*), the adsorption of *m*-xylene on dehydrated zeolite LaNaY (sample 12) causes a signal with a peak at −20 ppm (denoted as QL). The second-order quadrupolar shift of this ^{23}Na MAS NMR signal recorded at magnetic field strengths of $B_0 = 9.4$ T and 11.7 T yields a χ value of 2.4 ± 0.2 MHz. The numbers of sodium cations responsible for the components GL, QL and QP in the ^{23}Na MAS NMR spectrum of sample 12, calculated from the total number of Na^+ and the corrected relative ^{23}Na MAS NMR intensities, are given in the last row of Table 5. While the population of sodium cations on position SI is unaffected by adsorption of *m*-xylene, the number of sodium cations responsible for signal QP decreased from 14.9 Na^+ per uc (sample 11) to 5.7 Na^+ per uc (sample 12). Since the quadrupole coupling constant of signal QP in the spectrum of sample 12 was determined to be 3.6 ± 0.2 MHz, this signal should originate from sodium cations located on position SII in the large cavities (see ref. 35). In addition, 9.1 Na^+ per uc are strongly affected by the guest molecules and show a decrease of the χ value from about 4.2 MHz (signal QP) to about 2.4 MHz (signal QL). Also, these sodium cations must be located in the large cavities. Except for the 0.4 Na^+ per uc localized on position SI, therefore, all sodium cations in the dehydrated zeolite LaNaY loaded with *m*-xylene are located in the large cavities.

Discussion

Comparison of XRD and NMR Results

Reasonable agreement between XRD and NMR results was obtained in terms of the guest-molecule-induced sodium migration from sodalite cage to supercage, stability of the La^{3+} SI′ position, and the occupation of positions SII and SI′ mainly by sodium cations.

However, in some cases discrepancies were also noted. XRD yielded no population of site I by sodium, whereas the GL signal in the ^{23}Na MAS NMR spectra was attributed to this site. The most probable explanation for this discrepancy, however, is that the population of SI by sodium [0.5(5) Na^+ per uc] determined using ^{23}Na MAS NMR spectroscopy is too small to be detected by Rietveld refinement. This result demonstrates that ^{23}Na MAS NMR spectroscopy is a more sensitive method for the detection of sodium cations at sites with a small quadrupolar coupling constant than XRD using the Rietveld method.

Cation Migration during Calcination

The following picture of the migration of the lanthanum and sodium cations during calcination is obtained from a combination of the diffraction and spectroscopic results: Only the sodium cations in the supercage are replaced by lanthanum cations during the cation exchange.[4,7] The residual sodium cations are located in the small cavities of zeolite NaY. The cation migration starts between 323 and 363 K after desorption of water molecules. Since the diameter of the hydrated La^{3+} cations is 7.9 Å, and that of the six-ring window to the sodalite cage is 2.5 Å,[36] the loss of their hydration shell is a prerequisite for the migration of lanthanum cations into the sodalite cage. A complete removal of the water of hydration might be excluded because of the existence of at least one extra-framework oxygen atom bound to La^{3+} at position SI′ as shown by XRD and TG. The shedding of the hydration shell occurs simultaneously with the formation of Brønsted acid sites, which is well established in the literature.[9,12,37] At 393 K, the lanthanum cations already occupy position SI′ in the sodalite cage. This migration process is complete at *ca.* 473 K. The sodium cations migrate in the opposite direction to lanthanum from sodalite cage to supercage. All sodium cations are located at position SII in the supercage at 543 K. This migration of lanthanum and sodium is in general agreement with the results of other work.[4,6,7,9,10]

Rietveld analysis detected one extra-framework oxygen atom at position OW(1) in the sodalite cage. The distance from OW(1) to lanthanum at position SI′ is 2.4 Å, typical for a distance between a lanthanum ion and an oxygen atom and in agreement with previous results.[9,13] Approximately one extra-framework oxygen per lanthanum [exact value is 1.0 (3)] was obtained from the TG studies and the Rietveld analysis of the 543 K sample. This is in reasonable agreement with the results of Cheetham *et al.*[9] and Smith *et al.*[13] However, we localized the extra-framework oxygen at the specific position 96*g* and not at 32*e*[9,13] of space group $Fd\bar{3}m$. One possible explanation for this discrepancy is that Fourier sections often show an overestimated electron density at positions with high symmetry, as in the case of 32*e*. Secondly, the extra-framework oxygen atoms at OW(1) are statically disordered. Therefore, one extra-framework oxygen atom at position 32*e* could compensate for all of the electron density resulting from the oxygens at positions 96*g*.

Site I was not occupied in any of our samples, in contrast with the results of other authors.[8,38] However, Mortier and co-workers[38] have also found that their results are not comparable with those of other authors. They decided that it is not possible to derive definite conclusions if samples are compared for which the pretreatment conditions are not absolutely identical, especially since the cation mobility in zeolites is very low so that the equilibrium for dehydrated samples is often not reached. Therefore, the reason for the discrepancy with theoretical cation populations[39] calculated for equilibrium conditions is also obvious.

Cation Migration by Heating and after Guest-molecule Adsorption

From *ex situ* X-ray powder diffraction experiments a reversible, thermally induced sodium migration from the sodalite cages to position SII in the supercages (*cf.* Fig. 5) was identified. The lanthanum ions are not influenced by temperature. Such a reversible sodium migration has not been previously reported for zeolite Y.

Guest-molecule adsorption (*m*-xylene) also causes sodium migration from the sodalite cages to position SII. This was observed by both X-ray powder diffraction [*cf.* Fig. 4(*b*)] and

Published on 01 January 1995 on http://pubs.rsc.org | doi:10.1039/FT9959101813
Downloaded by Universitat Stuttgart on 20 June 2012

View Online

Published on 01 January 1995 on http://pubs.rsc.org | doi:10.1039/FT9959101813
Downloaded by Universitat Stuttgart on 20 June 2012

^{23}Na MAS NMR spectroscopy (*cf.* Fig. 10). In addition, both methods [*cf.* Fig. 4(*a*) and Fig. 8, 9] showed no influence of the guest molecule on the lanthanum cations at position SI′. Before and after guest-molecule adsorption, all lanthanum ions remain at position SI′ in the sodalite cage.

These results are in reasonable agreement with literature data and it might be concluded that the highly charged rare-earth-metal cations remain in the sodalite cage after their first migration from supercage to sodalite cage. Czjzek *et al.*[19,40,41] localized aromatic guest molecules in an ytterbium-exchanged zeolite NaY. It could be shown that the ytterbium cations were always in the sodalite cage at position SI′ and were not influenced by the guest molecule. Sodium migration was also noted by Klein *et al.*,[26] who showed that the adsorption of *m*-dinitrobenzene leads to the occupation of position SIV in the centre of the supercage by sodium. Nickel migration from sodalite cage to supercage was observed in NiNaY[42,43] during the activation step, where the zeolite was treated with small molecules like acetylene or hydrogen. This Ni^{2+} migration indicates that there must be a particular reason, perhaps a rare-earth-metal cluster,[7,10,37] for the stability of the rare-earth-metal cations at position SI′.

Cations and Guest Molecules in Conditions similar to those of Catalysis

In situ investigations of the structure of calcined zeolite LaNaY gave the same results as *ex situ* measurements. All sodium cations are located at position SII, whereas all lanthanum cations are situated at position SI′ in the sodalite cage. Passing *m*-xylene over the active catalyst causes no change in the zeolite structure. The guest molecule *m*-xylene could be located, even at temperatures of up to 623 K, in the region of the cation adsorption site. This is in agreement with molecular dynamics (MD) simulations of benzene and *p*-xylene in zeolite NaY.[44] Analysis of one-particle trajectories showed that the residence probability of the aromatic molecules in the region of the cation adsorption site is *ca.* 90% at 700 K. The rotational and translational disorder of *m*-xylene around this position is high, if we consider further results of this MD simulation and the results of quasi-electric neutron scattering experiments.[45] Therefore, our diffraction results show that the centre of mass of *m*-xylene is located at the preferred adsorption site. Rotation about the six-fold axis and vibration of the centre of mass presumably occur.

Conclusions

We have demonstrated the complementary nature of X-ray powder diffraction and multinuclear solid-state NMR spectroscopic experiments. Based on these methods, a migration mechanism for lanthanum and sodium during calcination could be derived. Above 423 K, lanthanum cations are situated only at SI′ in the sodalite cage. This position is stable and not influenced by temperature and guest-molecule adsorption. A guest-molecule- and temperature-induced sodium migration, however, was observed.

The structure of zeolite LaNaY obtained from *ex situ* measurements is very similar to that obtained by *in situ* studies. Structural data obtained from *ex situ* diffraction studies can therefore describe the structure of the active catalyst. The transferability to other systems is at present under study.

We acknowledge the Technische Hochschule Darmstadt for the provision of a grant for H.K. The authors also gratefully acknowledge support from the Fonds der Chemischen Industrie, Frankfurt, the Bundesministerium für Forschung und Technologie, the Deutsche Forschungsgemeinschaft, and the Max Buchner-Forschungsstiftung, Frankfurt. Furthermore, we are indebted to Prof. J. Weitkamp (Institute of Chemical Technology I, University of Stuttgart), for enabling the NMR measurements on the Bruker MSL 400 spectrometer, and Dr. G. Engelhardt for helpful comments (Institute of Chemical Technology I, University of Stuttgart).

References

1 *Fluid Catalytic Cracking*, ed. M. L. Occelli, American Chemical Society, Washington DC, 1988.
2 I. Halasz, J. Horvath, T. Mandy, L. Schmidt and E. Tasnadi, in *Proc. Int. Symposium on Zeolites, Portoroze, 1984*, ed. B. Držaj, S. Hočevar and S. Pejovnik, Elsevier, Amsterdam, 1985, p. 393.
3 H. S. Sherry, *J. Colloid Interface Sci.*, 1969, **28**, 288.
4 E. F. T. Lee and L. V. C. Rees, *Zeolites*, 1987, **7**, 143.
5 M. Hunger, G. Engelhardt and J. Weitkamp, *Microporous Mater.*, in the press.
6 E. F. T. Lee and L. V. C. Rees, *Zeolites*, 1987, **7**, 545.
7 P. Marynen, A. Maes and A. Cremers, *Zeolites*, 1984, **4**, 287.
8 D-S. Shy, S-H. Chen, J. Lievens, S-B. Liu and K-J. Chao, *J. Chem. Soc., Faraday Trans.*, 1991, **87**, 2855.
9 A. K. Cheetham, M. M. Eddy and J. M. Thomas, *J. Chem. Soc., Faraday Trans. 1*, 1984, **80**, 1337.
10 W. Grünert, U. Sauerlandt and H. G. Karge, *J. Phys. Chem.*, 1993, **97**, 1413.
11 M. Hunger, G. Engelhardt and J. Weitkamp, *Proc. 10th Int. Zeolite Conf., 1994, Garmisch-Partenkirchen*, Elsevier, Amsterdam, 1994, p. 725.
12 J. W. Ward, *J. Catal.*, 1969, **13**, 321.
13 J. V. Smith, J. M. Bennett and E. M. Flanigen, *Nature (London)*, 1967, **215**, 241.
14 G. R. Eulenberger, D. P. Shoemaker and J. G. Keil, *J. Phys. Chem.*, 1967, **71**, 1812.
15 D. H. Olson, *J. Phys. Chem.*, 1968, **72**, 4366.
16 A. N. Fitch, H. Jobic and A. Renouprez, *J. Phys. Chem.*, 1986, **90**, 1311.
17 W. J. Mortier, *Compilation of Extra-Framework Sites in Zeolites*, Butterworth, Guildford, 1982.
18 J. V. Smith, *Adv. Chem. Ser.*, 1971, **101**, 171.
19 M. Czjzek, H. Fuess and T. Vogt, *J. Phys. Chem.*, 1991, **95**, 5255.
20 M. R. Basila, T. R. Kantner and K. H. Rhee, *J. Phys. Chem.*, 1964, **68**, 3197.
21 H. M. Rietveld, *J. Appl. Crystallogr.*, 1969, **19**, 92.
22 F. Izumi, *Nippon Kesshyo Gakkai-Shi*, 1985, **27**, 23.
23 F. Izumi, *The Rietveld Method*, ed. R. A. Young, Oxford University Press, Oxford, 1993, ch. 13.
24 A. Zalkin, FORDAP, A FORTRAN Program for Fourier Calculations, University of California, Berkeley, 1965.
25 D. W. Breck and E. M. Flanigen, in *Molecular Sieves*, Soc. Chem. Ind., London, 1968, p. 47.
26 H. Klein, C. Kirschhock and H. Fuess, *J. Phys. Chem.*, 1994, **98**, 12345.
27 G. Engelhardt and D. Michel, *High-Resolution Solid-State NMR of Silicates and Zeolites*, Wiley, Chichester, 1987.
28 K-J. Chao and J-Y. Chern, *J. Phys. Chem.*, 1989, **93**, 1401.
29 G. Engelhardt and W. Veeman, *J. Chem. Soc., Chem. Commun.*, 1993, 622.
30 H. K. Beyer, G. Pal-Borbely and H. G. Karge, *Microporous Mater.*, 1993, **1**, 67.
31 B. Welsh and S. L. Lambert, in *Perspectives in Molecular Sieve Science*, ed. W. H. Flank and T. E. Whyte, American Chemical Society, Washington DC, 1988, p. 33.
32 C-F. Lin and K-J. Chao, *J. Phys. Chem.*, 1991, **95**, 265.
33 D. Massiot, C. Bessada, J. P. Coutures and P. Taullelle, *J. Magn. Reson.*, 1990, **90**, 231.
34 M. Hunger, G. Engelhardt, H. Koller and J. Weitkamp, *Solid-State Nucl. Magn. Reson.*, 1993, **2**, 111.
35 G. Engelhardt, M. Hunger, H. Koller and J. Weitkamp, *Stud. Surf. Sci. Catal.*, 1994, **84**, 421.
36 C-F. Lin and K-J. Chao, *J. Phys. Chem.*, 1991, **95**, 9411.
37 M. L. Poutsma, *Zeolite Chemistry and Catalysis*, ACS Monographs, 1976, **171**, 437.
38 W. J. Mortier, E. Van den Bossche and J. B. Uytterhoeven, *Zeolites*, 1984, **4**, 41.
39 J. J. Van Dun and W. J. Mortier, *J. Phys. Chem.*, 1988, **92**, 6740.

View Online

40 M. Czjzek, T. Vogt and H. Fuess, *Zeolites*, 1991, **11**, 832.
41 M. Czjzek, T. Vogt and H. Fuess, *Zeolites*, 1992, **12**, 237.
42 J. W. Couves, R. H. Jones, J. M. Thomas and B. J. Smith, *Adv. Mater.*, 1990, **2**, 181.
43 E. Doorhye, C. R. A. Catlow, J. W. Couves, P. W. Maddox, J. M. Thomas, G. N. Greaves, A. T. Steel and R. P. Townsend, *J. Phys. Chem.*, 1991, **95**, 4514.
44 H. Klein, H. Fuess and J. Brickmann, submitted.
45 M. Czjzek, H. Jobic and M. Bee, *J. Chem. Soc., Faraday Trans.*, 1991, **87**, 3455.

Paper 4/07726A; *Received* 19*th December*, 1994

Downloaded by Universitat Stuttgart on 20 June 2012
Published on 01 January 1995 on http://pubs.rsc.org | doi:10.1039/FT9959101813